Pertanika J. Sci. & Technol. 31 (4): 2123 - 2143 (2023)

PERTANIKA JOURNALS

SCIENCE & TECHNOLOGY

Journal homepage: http://www.pertanika.upm.edu.my/

Self-Consistent Positive Streamer-Leader Propagation Model Based on Finite Element Method (FEM) and Voltage Distortion Method (VDM)

Ziwei Ma, Jasronita Jasni*, Mohd Zainal Abidin Ab Kadir and Norhafiz Azis

Department of Electrical and Electronic Engineering, Faculty of Engineering, Universiti Putra Malaysia, 43400 UPM, Serdang, Selangor, Malaysia

ABSTRACT

Researchers have worked on positive leader propagation models and proposed different theoretical and numerical approaches. The charge simulation method (CSM) has traditionally been chosen to model the quasi-static electric field of each stage of leader propagation. The biggest drawback of the CSM is that the calculation is complicated and time-consuming when dealing with asymmetric electric field structures. On the contrary, the finite element method (FEM) is more suitable and reliable for solving electrostatic field problems with asymmetric and complex boundary conditions, avoiding the difficulties of virtual charge configuration and electric field calculation under complex boundary conditions. This paper modeled a self-consistent streamer-leader propagation model in an inverted rod-plane air gap based on FEM and the voltage distortion method (VDM). The voltage distortion coefficient was analyzed to calculate the streamer length and space charge. The physical dynamic process of the discharge was simulated with the help of COMSOL Multiphysics and MATLAB co-simulation technology. The results show that the initial voltage of the first corona is -1036 kV, close to the experiment value of -1052 kV. The breakdown voltage of -1369 kV is highly consistent with the experimental value of -1365 kV. The largest streamer length is 2.72 m, slightly higher than the experimental value of 2.3 m. The leader velocity is 2.43×104 m/s, close to the experiment value of 2.2×104 m/s. This model has simple calculations and can be used in complex electrode configurations and arbitrary boundary conditions without simplifying the model structure, making the model more flexible.

Keywords: COMSOL, FEM, leader progression model, space charge, streamer, voltage distortion method

ARTICLE INFO

Article history:
Received: 22 August 2022
Accepted: 14 November 2022
Published: 13 June 2023

DOI: https://doi.org/10.47836/pjst.31.4.30

E-mail addresses:
GS59360@student.upm.edu.my (Ziwei Ma)
jas@upm.edu.my (Jasronita Jasni)
mzk@upm.edu.my (Mohd Zainal Abidin Ab Kadir)
norhafiz@upm.edu.my (Norhafiz bin Azis)
* Corresponding author

ISSN: 0128-7680
e-ISSN: 2231-8526

INTRODUCTION

Long-gap discharge experiments under various electrode structures carried out by Les Renardières Group (1972, 1974) have made people systematically recognize the phenomenon and characteristics of the leader discharge. Based on the understanding of the physics of leader inception and development, the leader propagation method (LPM) was introduced to simulate the process of leader discharge in the 1970s. In engineering applications, such as lightning protection design, LPM is recommended as a more physically reasonable method to evaluate the lightning protection performance of grounded structures under the influence of lightning downward leader (Cigre, 2021). Theoretical approaches and numerical models of positive leader discharge based on LPM have been developed in the past few decades.

Rizk (1989) developed a mathematical model for stable leader inception and breakdown of rod-plane gaps under positive switching impulse voltage based on the basic theory of the electrostatic field. This model was successfully extended to conductor-plane gaps and could predict the 50% breakdown voltage for a wide range of air spacing. However, this model cannot simulate the dynamic process of leader development.

Bondiou and Gallimberti (1994) proposed a self-consistent leader inception and propagation model (SLIM) based on the mass, momentum, and energy conservation equations. In this model, the output of each discharge stage is used as the next stage's input, and the input parameters are only the electrode geometry and the applied voltage waveform. However, the model involves many physical parameters, making the calculation process complex.

Based on the Bondiou & Gallimberti model, Goelian et al. (1997) introduced a numerical model to calculate the space charge and the streamer length using the voltage distortion method (VDM). However, the function used to calculate the streamer space charge is related to the electrode structure and to the streamers' length, number, and radius. So, the calculation process is much more complicated. At the same time, the model only considers the case where the electrode voltage is constant, while the electrode voltage is a constantly changing voltage in most actual situations.

Becerra and Cooray (2006a) proposed a simplified self-consistent upward leader model-based VDM. In this model, the calculation of streamer space charge is simplified by using the electrode geometry coefficient K_Q multiplied by the area difference between the background voltage U_1 and the streamer voltage U_2. However, the model chooses the geometric coefficient K_Q as a constant value and does not further analyze the factors affecting K_Q. In addition, to simplify the calculation, the model replaces the distribution of the background voltage U_1 with a straight-line segment, exaggerating the areas enclosed by U_1 and U_2 so that the calculated space charge of the streamer may be larger than the actual value. Simplified VDM proposed by Becerra and Cooray (2006a) is widely used in leader discharge simulation, such as the research done by Mohammadi et al. (2019) and Gu et al. (2020).

The models mentioned above use the charge-simulated method (CSM) to calculate the electric field distribution generated by the applied voltage and streamer space charge. The disadvantage of the CSM is that the calculation process will become so sophisticated when encountering asymmetric and complex electric field structures that the computation time and computational memory requirements become large. Because of this, it is often necessary to simplify the complex electric field structure into a simple structure, leading to a large error between the calculated and actual results. For the problem of the electrostatic field, the finite element method (FEM) is a more effective and reliable method for the electrostatic boundary value problems. Especially when dealing with asymmetric electrode structures and complex boundary conditions in practical engineering, FEM can take advantage of its faster calculation speed and higher calculation accuracy. The research done by Talaat et al. (2019), Becerra (2013), Zhou et al. (2018), and Diaz et al. (2018) has proved that.

Today's advancement of FEM commercial software, such as COMSOL, has multiphysics coupling functions and powerful computing capabilities and has been widely used in engineering applications and scientific research. For example, Gao et al. (2020), Hnatiuc et al. (2019), Brezmes and Breitkopf (2014), and Arevalo et al. (2012) used COMSOL Multiphysics to simulate the discharge process in air. Rodrigues et al. (2019), Yang et al. (2017), Chen et al. (2016), and Xu and Chen (2013) used COMSOL Multiphysics to research the characteristics of lightning strike protection in engineering.

The main goal of this paper is to develop a positive self-consistent leader Inception and propagation model of an inverted rod plane under the switching impulse voltage based on the latest physical knowledge obtained in DC discharge experiments. The calculation adopts the FEM and the VDM to calculate the streamer length and steamer space charge at every step of the discharge process. Based on the previous calculation, the velocity and the length of the leader, the length of the final jump, and the breakdown voltage can be calculated. The model can complete the self-iterative calculation through COMSOL and MATLAB co-simulation technology. The validity of this model can be verified by comparing it with experimental results in the literature. Ultimately, this numeric model will be extended to simulate the development process of the positive upward leader generated from EHV TLs under the impact of the lightning downward leader so that the lightning shielding performance of EHV TLs can be evaluated.

INPUT PARAMETERS AND METHODOLOGY

Design Parameters for Simulation Model

In order to verify the validity of the simulation, the size of the simulation model is the same as the actual experimental model (He et al., 2012). The electrode system of the model is an inverted rod-plane structure (Figure 1). The plane electrode is suspended in the air

at 5 m above the ground and is connected to the generator of switching impulse voltage. The rod electrode covered with a spherical head is placed on the grounded and directly grounded. A negative standard switching impulse voltage with an amplitude of 1500 kV is applied to the plane electrode. The geometric parameters and applied voltage of the experimental setup are shown in Table 1.

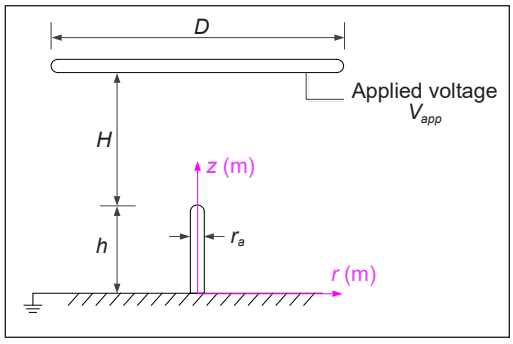

Figure 1. The inverted rod-plane electrode structure of the experiment

Table 1
Geometric parameters and applied voltage of the simulation model

Parameter item	Parameter value	Unit
The height of the rod h	2	m
The radius of the rod r_a	15	cm
The length of the air gap H	3	m
The side length of plane D	6	m
The amplitude of the applied voltage V_{app}	1500	kV
The wavefront/tail time of V_{app} T_f/T_t	250/2500	μs

Simulation Modeling

A 2D symmetrical model is built in COMSOL Multiphysics (Figure 2). The boundary conditions are constrained: 1 is a high voltage boundary, 2 and 3 are zero potential, and 4 is an infinite element domain. The infinite element domain replaces the infinitely extending space around the electrode system. The electric field does not change abruptly on the inner boundary of the infinite element domain, while on the outer boundary of the infinite domain, the electric potential is zero. The model is symmetric, so only half of the computational domain is shown in Figure 2.

Meshing is the key to FEM calculation. The index for judging the quality of meshing is the element quality. COMSOL provides seven element quality measurement tools: skewness, maximum angle, volume versus circumradius, volume versus length, condition number, growth rate, and bending skewness. Skewness is suitable for most mesh types and is adopted as the measurement tool of mesh quality for this

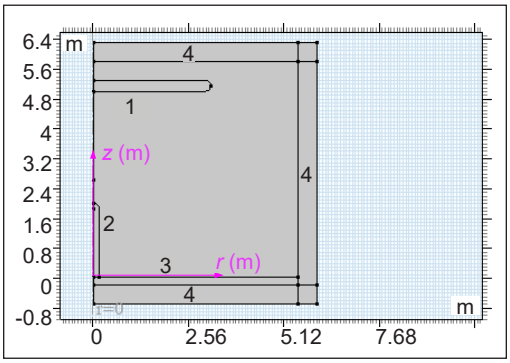

Figure 2. 2D axisymmetric simulation model

model. Skewness refers to the degree of closeness between the mesh element and the equal-angle ideal element. The calculation method is shown in Equation 1, where θ_e is the vertex angle of the ideal element, and θ is the vertex angle of the divided mesh element, as shown in Figure 3. Green represents the high-quality meshes, and red represents the low-quality meshes. The mesh element quality measure is between 0 and 1, with 1 being extremely high quality and 0 being extremely poor quality. The criteria for the mesh element quality are shown in Table 2.

$$Skewness = 1 - \max\left(\frac{\theta - \theta_e}{180 - \theta_e}, \frac{\theta_e - \theta}{\theta_e}\right) \quad [1]$$

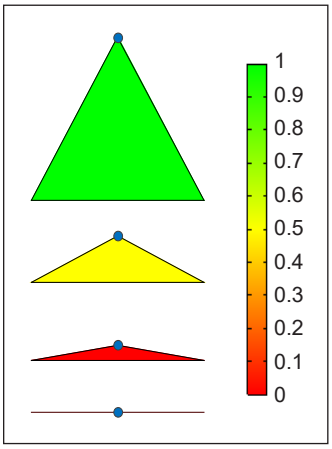

Figure 3. Schematic diagram of mesh skewness measurement

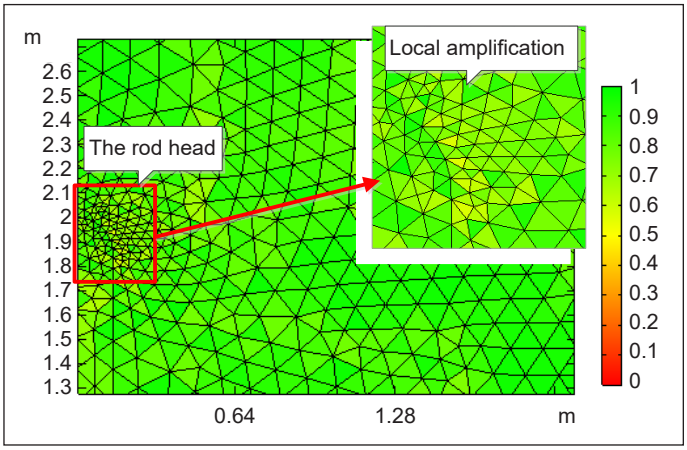

Figure 4. Mesh element quality in rod head region in a 2D axisymmetric model

Adaptive meshing is used in this model. Except for the infinite element domain, which uses a regular quadrilateral mesh, the rest of the domains are all triangular meshes. The mesh quality of the rod electrode head, which is of most concern, is shown in Figure 4. The curvature of the rod electrode head is large, so the quality of the mesh element is relatively poor, as shown in the yellow part in Figure 4.

Table 2
The criteria for the mesh element quality

Skewness	Mesh element quality
< 0.02	Extremely poor
0.02 ≤ Skewness < 0.2	Poor
0.2 ≤ Skewness < 0.35	Basic
0.35 ≤ Skewness < 0.75	Medium
0.75 ≤ Skewness < 1	High
1	Extremely high

After applying a locally refined mesh to the rod electrode head region, the number of low-quality elements is reduced (Figure 5). From the mesh statistics, after local refinement, the minimum and average element quality are improved (Table 3). The average element quality of this model is above 0.9, indicating that the mesh quality is high.

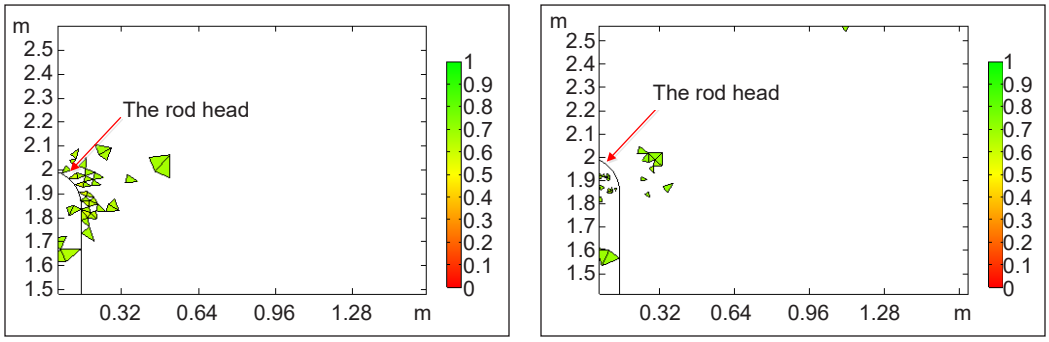

Figure 5. Comparison of mesh element quality before and after mesh refinement in the region of the rod head: (a) Before mesh refinement; and (b) After mesh refinement

Table 3
Meshing statistics of the 2D axisymmetric model

Mesh parameters	Before refinement	After refinement
Number of elements	6030	7117
Number of triangle elements	5365	6452
Number of quadrilateral elements	665	665
Minimal element quality	0.5503	0.5836
Average element quality	0.9102	0.9152

The Streamer-Leader Propagation Model

Many experimental studies have shown that the positive leader discharge process consists of five stages: initial streamer formation, streamer-leader transition, streamer-leader system development, final jump, and gap breakdown. If the radius of the positive electrode is larger than the critical radius, a stable streamer-leader discharge system can be generated after the initial corona (Les Renardières Group, 1972, 1974). This model does not cover the case where the radius of the positive electrode is smaller than the critical radius.

The theory of positive streamer discharge holds that the applied external electric field supplies the energy to generate the primary electron avalanche on the surface of the positive electrode (Nijdam et al., 2020). When the number of positive charges of the primary avalanche is greater than the critical value of 10^8 (Naidu & Kamaraju, 2013), the electric field generated by these charges is equivalent to the external applied electric field will induce secondary electron avalanches near the anode electrode. The secondary electron avalanches are attracted to the tail of the main avalanche, and the electrons are absorbed, leaving the newly generated positive charges in the tail of the main avalanche. This process continues to repeat, thus forming a streamer that develops from the anode to the cathode. It is generally considered that the critical field strength of the positive streamer inception is 2600 kV/m (Cooray, 2014; Gallimberti et al., 2002).

After the initial streamer is formed, multiple branched streamers in a dendritic shape are formed during its development. The free electrons generated by the branched streamers flow into the anode through the common streamer stem. As the streamers' current increases, the streamers' stem is heated. When the temperature exceeds 1500 K, thermal ionization greatly increases the electrical conductivity at the streamer stem, which turns the streamer stem into a high-temperature and high-conductivity leader channel (El-Zein et al., 2018; Gallimberti et al., 2002).

The field strength in the leader channel is relatively low, generally considered 30–50 kV/m (Becerra & Cooray, 2006a; Rizk, 2009). When the leader channel extends forward, most of the voltage of the anode is transmitted to the leader's head through the leader channel, which is equivalent to the forward extension of the anode. When the field strength of the leader's head reaches the critical intensity of air discharge, a new streamer is generated. This process is repeated to form a streamer-leader discharge development system (Figure 6). As the leader travels from the previous streamer zone, the streamer space charges form a corona sheath around the leader channel. Whether the leader can continue to develop depends on whether the streamer discharge at the leader's head can continuously provide energy to maintain the thermal ionization of the leader channel.

When the streamer at the head of the leader reaches the cathode, the final jump occurs. As a result, the leader channel quickly bridges the remaining gap, and a strong short-circuit current flows through the leader channel to break down the entire gap.

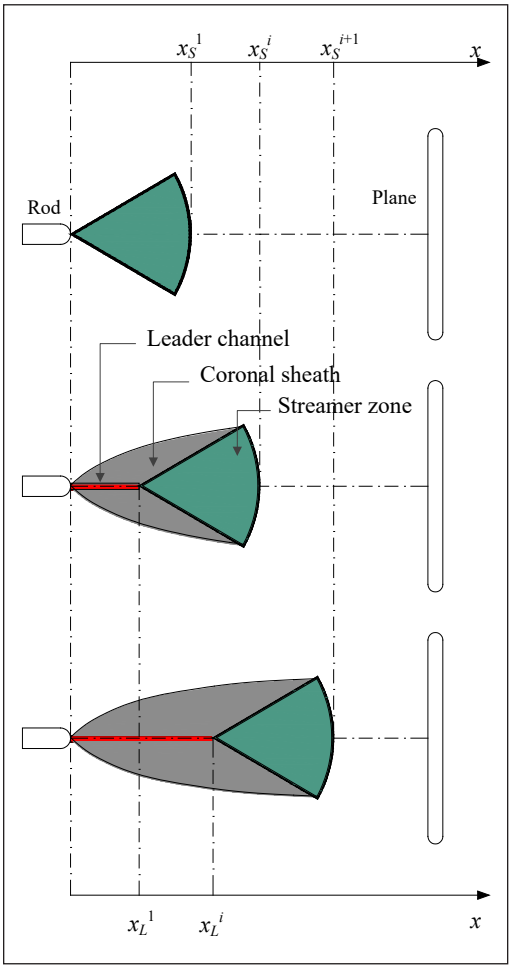

Figure 6. Schematic diagram of the streamer-leader system development

The Calculation of the Initial Streamer Length and Streamer Space Charge

The potential distribution generated by the applied voltage in the rod-plate gap is an exponential distribution curve, referred to as the potential background V_1 for short. During the streamer development, the streamer space charge will cause electric field distortion

in the gap between the electrodes. It is generally considered that the electric field inside the streamer zone is constant, and the value is about 450 kV/m–500 kV/m (Ding et al., 2016; Rizk, 2020; Petrov & Waters, 2021). Therefore, the voltage distribution in the streamer region is a linear curve, referred to as the streamer potential V_2 for short. The difference between these two voltage curves can calculate the degree of voltage distortion. In this way, the voltage distortion method (VDM) can be used to calculate the streamer length and space charge (Figure 7).

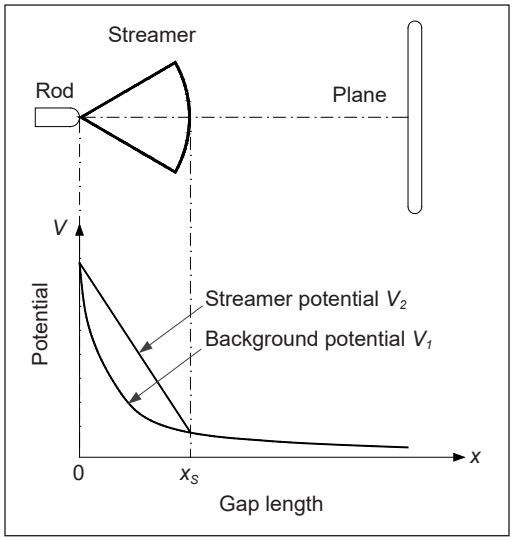

Figure 7. Calculation of streamer length and streamer space charge by VDM

The horizontal axis x in Figure 7 is the gap length, and the vertical axis V is the potential in the gap. The abscissa length x_s corresponding to the intersection of V_1 and V_2 is the length of the initial streamer. The streamer space charge can be calculated by multiplying the area A enclosed by the two curves by the voltage distortion coefficient K_Q (Equation 2).

$$Q = K_Q A = K_Q \int_0^{x_s} (V_2 - V_1) dx \qquad [2]$$

The Calculation of the Subsequent Streamer-Leader System

For this simulation model, the rod electrode radius is 15 cm, greater than the critical radius of 12.5 cm (He et al., 2012). Therefore, a stable development leader can be formed once the initial streamer is generated, which is also confirmed by the experiments (He et al., 2012). The discharge develops in a stepwise fashion. As mentioned earlier, continuous leader development depends on the charge provided by the streamer discharge at the head of the leader. The step length of the leader can be calculated by Equation 3 (Becerra & Cooray, 2006b), where Q_i is the space charge generated at ith step discharge in μC, τ is the charge density of the leader channel in μC/m.

$$l_L{}^i = \frac{Q_i}{\tau} \qquad [3]$$

Regarding the charge density of the positive leader channel, Gallimberti et al. (2002) considered it to be 20–50 μC/m. Petrov and Waters (2021) considered it to be 20 μC/m. Rizk (1989) and Becerra and Cooray (2006b) considered it 45–50 μC/m. Experiments by Wang et al. (2016) also indicated that the positive leader channel's charge density is 40–50

μC/m. Li et al. (2013) experiments confirmed the charge densities in the 30–50 μC/m. The experiments of Zeng et al. (2013) showed that the charge density is 30–70 μC/m. By artificially triggered lightning experiments, Lalande et al. (2002) observed a positive leader charge density of 65 μC/m. In this paper, the charge density of the positive leader channel is 25 μC/m.

The diameter of the leader channel is generally considered to be several millimeters, and this model takes 2 mm. The leader channel's voltage drop is calculated using Equation 4, where E_L is the average field strength of the leader channel in kV/m, and $l_L{}^i$ is the step length of the leader development to the ith step. The leader channel E_L's average field strength is 50 kV/m.

$$V_L{}^i = E_L l_L{}^i \qquad [4]$$

The velocity of the positive streamer development is on the order of 10^5 m/s. The experiments of Ding et al. (2016) and He et al. (2012) show that the average development speed of the positive streamer is 1×10^5 m/s. Cooray (2014) considered it to be 2×10^5 m/s. However, Nijdam et al. (2020) considered the velocity of the streamer to be on the order of 10^5–10^6 m/s. In this paper, the positive streamer's average velocity is assumed to be 1×10^5 m/s.

The potential distribution in the gap during the streamer-leader propagation is shown in Figure 8. $V_L{}^{i-1}$ is the voltage drop of the leader channel at step i-1. $V_2{}^{i-1}$ is the streamer voltage at step i-1. Once a new streamer is generated at the head of the leader channel, the streamer voltage decreases to $V_2{}^i$ due to the voltage clamping of the leader channel. The shaded area in Figure 8 is the area of voltage distortion caused by the newly generated streamer space charge. The newly generated streamer space charge can be calculated by multiplying this part of the area by the voltage distortion coefficient K_Q. The abscissa intersection $x_S{}^i$ of the two curves $V_1{}^i$ and $V_2{}^i$ is the position of the new streamer head, and the length of the new streamer can

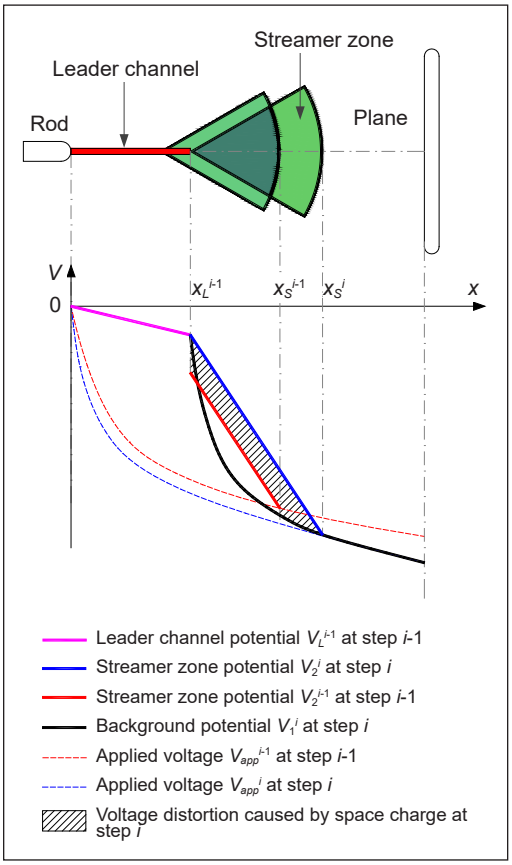

Figure 8. The streamer-leader system propagation and the potential gap distribution at step i

be obtained by subtracting the length of the leader channel V_L^{i-1} from x_S^i. V_{app}^{i-1} and V_{app}^{i} are the applied voltage on the plane at step i-1 and step I, respectively.

The streamer space charge at step i can be calculated by using Equation 5. x_L^{i-1} represents the leader channel length at step i-1. x_S^{i-1} and x_S^{i} represent the position of the streamer head at steps i-1 and i, respectively.

$$Q_i = K_Q \int_{x_L{}^{i-1}}^{x_S{}^{i-1}} \left(V_2{}^{i} - V_2{}^{i-1}\right) \mathrm{d}x + K_Q \int_{x_S{}^{i-1}}^{x_S{}^{i}} \left(V_2{}^{i} - V_1{}^{i}\right) \mathrm{d}x \quad [5]$$

This model only needs to input the electrode parameters and apply voltage waveform to simulate the dynamic process of streamer-leader propagation. Using the co-simulation technology of COMSOL Multiphysics and MATLAB, the streamer-leader size and applied voltage amplitude of each step of the discharge process can be calculated in MATLAB according to the voltage distribution of V_1 and V_2 output by the COMSOL model. The output of the previous step of the simulation is used as the input of the next step, and the model can realize self-iterative calculation. The simulation flowchart is shown in Figure 9.

RESULTS

The Critical Inception Voltage of the Streamer

Before the initial streamer is generated, there is no free-charge distribution in the plane-rod gap. The voltage distribution in the air gap is a Laplace function (Equation 6), where V is a scalar potential distribution function.

$$-\nabla^2 V(x, y, z) = 0 \quad [6]$$

At the boundary, the potential is constant. For the high-voltage electrode, the potential is the applied voltage (Equation 7), and for the ground electrode, the potential is 0 (Equation 8).

$$V(x, y, z) = V_0 \quad [7]$$

$$V(x, y, z) = 0 \quad [8]$$

Given the boundary potential, the problem of finding the spatial electric field distribution is the Dirichlet boundary problem. Due to the uniqueness of the electric field distribution, the unique function of the spatial potential distribution can be obtained by solving the Laplace Equation 6. The electric field strength vector is the negative value of the gradient of the scalar potential function; that is, the relationship of Equation 9 is satisfied. Based on these basic equations, the electric field distribution in the inverted rod-plane gap is calculated.

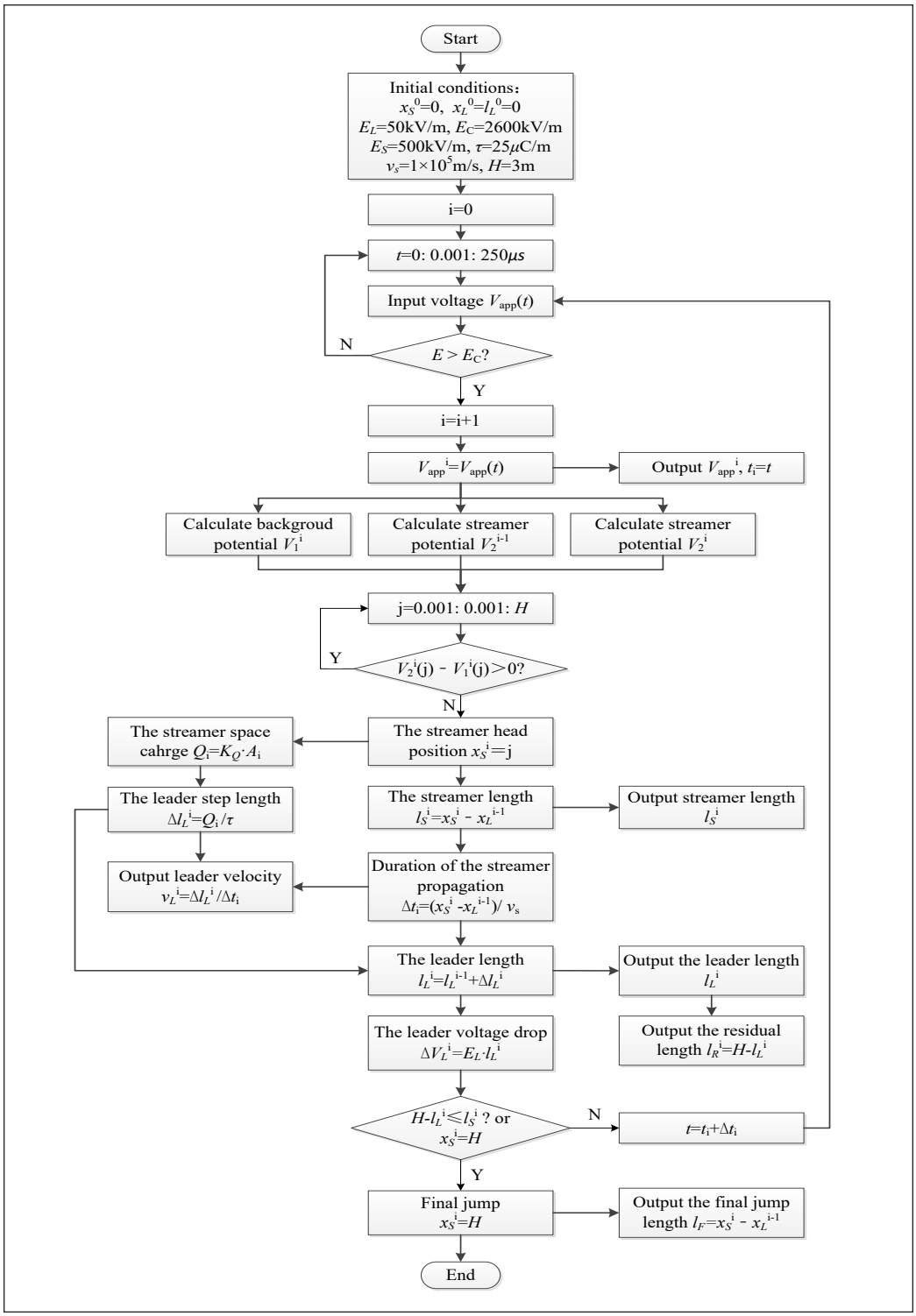

Figure 9. The simulation flowchart of the streamer-leader propagation model

$$\vec{E}(x,y,z) = -\nabla V(x,y,z) \quad [9]$$

The input voltage is a 250/2500 μs switching impulse voltage formed by a double exponential function with an amplitude of 1500 kV (Figure 10). With the gradual increase of the applied voltage, the electric field strength on the surface of the rod electrode increases gradually. When the electric field intensity reaches the critical electric discharge intensity of 2600 kV/m, the initial streamer is generated, and this moment is taken as the first step of the simulation process.

The simulation result shows that when the applied voltage of the plane electrode is increased to -1036 kV, the electric field strength on the surface of the rod electrode reaches the critical field strength of 2600 kV/m (Figure 11). The critical inception voltage of the streamer obtained by the simulation is close to the experimental value of -1052 kV, which proves that the calculation result of COMSOL Multiphysics is reliable.

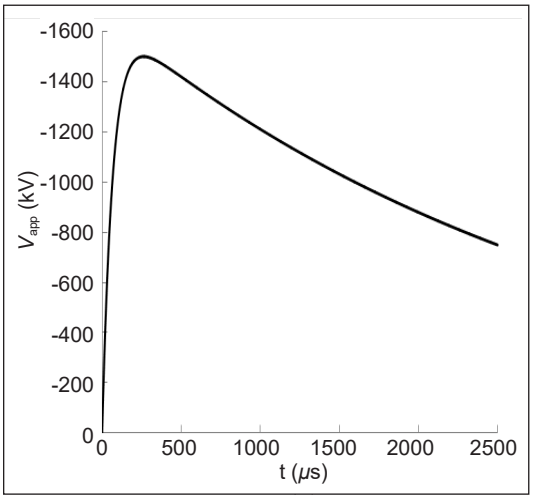

Figure 10. Switching impulse voltage waveform input by the simulation model

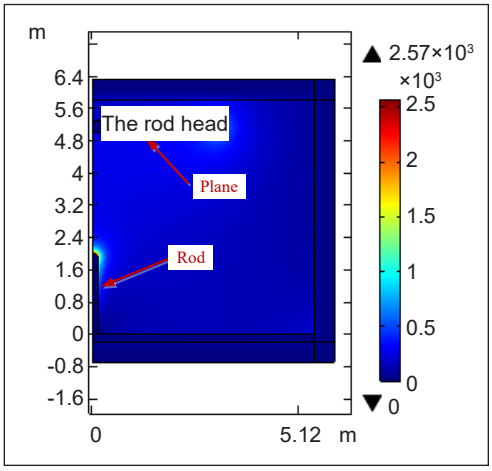

Figure 11. Electric field distribution in the 2D axisymmetric rod-plane gap under critical streamer inception voltage

The Initial Streamer Length and Streamer Space Charge

The selection of the coefficient K_Q is the key to calculating the streamer space charge. K_Q is related to the electrode structure (Becerra & Cooray, 2006a) and the streamer size (He et al., 2012). Becerra and Cooray's (2006a) model showed that the average value of K_Q is 0.035 μC/kV·m for the rod-plane electrode structure with a symmetric structure. The study by (He et al., 2012) shows that the K_Q value is in the range of (0.03-0.06) μC/kV·m. In this model, the back-calculation method is used, the space charge Q of the streamer is assumed in advance, and then the voltage distortion area A caused by the streamer space charge is calculated so that the distortion coefficient K_Q can be calculated from Equation

2. The calculation results show that K_Q is related to the gap and streamer lengths (Figure 12). With the increase of the gap distance, K_Q gradually decreases and tends to be saturated.

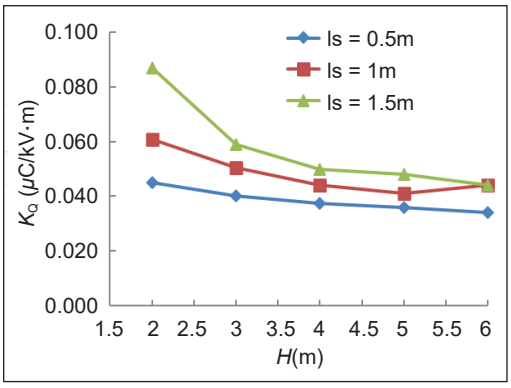

Figure 12. The relationship between K_Q and the gap distance and the length of the streamer under the negative plane-rod electrode structure

K_Q increases with the length of the streamer (Figure 12). Therefore, when using VDM to calculate the streamer space charge, different K_Q values should be selected according to the length of the streamer instead of taking a fixed average value as suggested by Becerra and Cooray (2006a) and He et al. (2012). The applied voltage and the gap length greatly affect the streamer length (Figure 13), where $V_1{}^i$ is the background potential generated by the electrode voltage, and $V_2{}^i$ is the streamer potential. The streamer length increases with the applied voltage for a certain gap length, as shown in Figure 13(a). The streamer length increases as the gap is shortened for a certain applied voltage, as shown in Figure 13(b). For this simulation model, the applied voltage to the plane electrode continues to increase until breakdown occurs. The gap length gradually decreases as the leader develops forward. Both trends will make the streamer longer. When the applied voltage exceeds -1350 kV, the streamer length can reach more than 2 m. Therefore, the value of K_Q should be between (0.04-0.08) μC/kV·m.

When the applied voltage reaches the critical corona onset voltage of 1036kV, the calculated initial streamer length is 1.04 m (Figure 13). K_Q should be taken as 0.05 μC/kV·m, from which the initial streamer space charge can be calculated to be 4.63 μC (Figure 12).

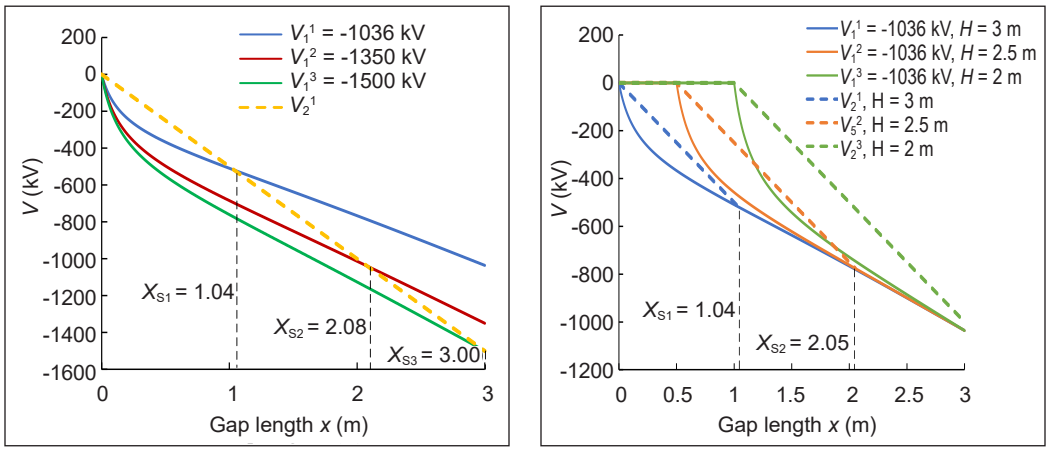

Figure 13. The effect of the: (a) applied voltage; and (b) gap length on the streamer length

Subsequent Streamer Length and Streamer Space Charge

The average speed of positive streamer propagation is assumed to be 1×10^5 m/s, from which the duration of the initial streamer can be calculated to be 10.4 μs. When the initial streamer propagation is completed, the applied voltage rises to -1117 kV. From Equation 3, the primary leader length can be calculated as 0.19 m. In the same way, as mentioned above, the secondary streamer length and streamer space charge can be calculated to be 1.41 m and 5.82 μC, respectively.

The subsequent streamer length and steamer space charge can be obtained by repeating the same calculation process (Figure 14). The final jump occurs after the streamer-leader system has developed 4 steps. In the final step, the background potential V_1^4 and the streamer potential V_2^4 do not intersect, which means that the head of the streamer has reached the plane electrode. It is generally believed that the final jump occurs when the head of the streamer reaches the opposite electrode (Cooray, 2014; Rizk, 1989). Thus, the final jump length can be obtained by subtracting the leader length from the gap length. The simulation results show that the final jump length is 2.04 m (Figure 14).

The macro parameters of each step of the leader discharge obtained by simulation are shown in Table 4. Before the final jump, the leader's velocity increases slightly with the leader's length. The average speed is about 2×10^4 m/s, close to the experiment result of 2.2×10^4 m/s (He et al., 2012). Once the final jump occurs, the leader velocity increases rapidly (Figure 15), where the abscissa l_L is the leader length, and the ordinate v_L is the leader speed. The variation trend of the leader speed is consistent with the experimental observation (He et al., 2012). The leader velocity of the final jump stage obtained by simulation is about 9.9×10^4 m/s, which is lower than the experiment results of 13.9×10^4 m/s but is highly close to the experiment result of 10×10^4 m/s observed by Les Renardières Group (1972, 1974).

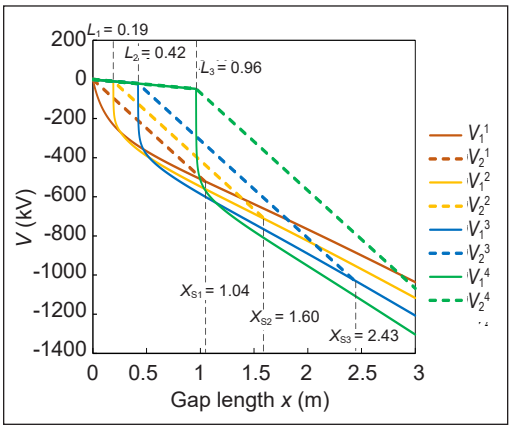

Figure 14. Gap potential distribution during the leader progression

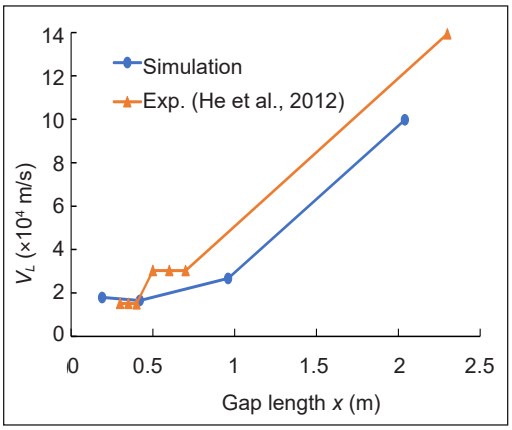

Figure 15. Comparison of the leader velocity simulation value and experimental value

Table 4
Simulation results of streamer-leader propagation system under the assumption of E_S=500 kV/m, τ=25 μC/m

Step	V_{app} (kV)	K_Q (μC/kV·m)	l_S (m)	Q (μC)	t (μs)	l_L (m)	v_L ($\times10^4$ m/s)	l_R (m)	Final jump
1	-1036	0.05	1.04	4.63	68.7	0.00	0.00	3.00	N
2	-1117	0.054	1.41	5.82	79.1	0.19	1.79	2.81	N
3	-1207	0.072	2.01	13.43	93.2	0.42	1.65	2.58	N
4	-1304	0.072	2.04	37.16	113.3	0.96	2.67	2.04	Y
5	-1374					2.04	9.98	0	Breakdown

V_{app} is the applied voltage on the plane electrode. K_Q is the voltage distortion coefficient. l_S is the streamer length. Q is the streamer space charge. t is the moment when the new streamer is generated. l_L is the leader length. v_L is the velocity of the leader propagation. l_R is the residual length of the gap.

The streamer length and streamer space charge increase in steps. Especially the streamer space charge increases sharply in the final stage.

The comparison between the simulation and the experimental results shows that the inception voltage of the initial streamer and the 50% breakdown voltage are in good agreement with the experiment results (Table 5). The maximum streamer length, the final jump length, and the leader velocity are slightly lower than the experimental results.

However, the duration of the streamer discharge process obtained by the simulation is quite different from the experimental results. The reasons may come from initial assumptions' influence, such as the charge density of leader channel τ, streamer voltage gradient E_S, and streamer velocity v_S. The effect of these parameters on the streamer discharge duration is shown in Figures 16 to 18, where the ordinate x_s is the height of the streamer head, and the abscissa T_d is the duration of streamer discharge. Reducing the charge density of the leader channel, reducing the streamer voltage gradient, or increasing the streamer velocity can reduce the discharge duration.

Table 5
The comparison between the simulation results and the experimental results under the assumption of E_S=500 kV/m, τ=25 μC/m

Parameters	Simulation results	Experimental results (He et al., 2012)	Unit	Error (%)
V_{ini}	-1036	-1052.00	kV	-1.5
l_{SM}	2.04	2.30	m	-11.3
l_F	2.04	2.30	m	-11.3
v_L	2.04	2.20	$\times10^4$ m/s	-7.3
T_d	44.6	29.7	μs	50.2
$V_{50\%}$	-1374	-1365.00	kV	0.7

V_{ini} is the critical inception voltage of the streamer. l_{SM} is the maximum streamer length. v_L is the average velocity of the leader propagation. T_d is the duration of the streamer discharge process. l_F is the length of the final jump. $V_{50\%}$ is the 50% breakdown voltage.

Based on the above analysis, two other simulations were carried out assuming that E_S=450 kV/m, τ=25 μC/m. The simulation results are shown in Table 6. The comparison between the simulations and experiment is shown in Table 7. Among the three simulations, the assumption of E_S=450 kV/m, τ=25 μC/m, and v_S=1×10^5 m/s yields the simulation results closest to the experimental values.

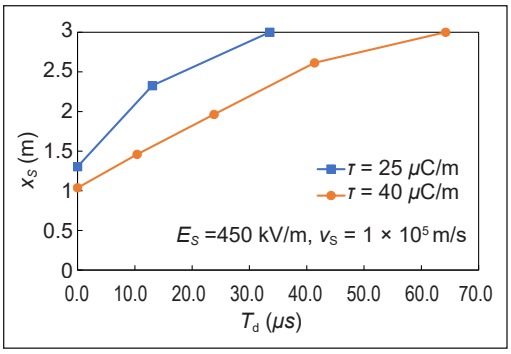

Figure 16. The effect of charge density τ on discharge duration under the assumption that E_S=450 kV/m, v_S=1×10^5 m/s

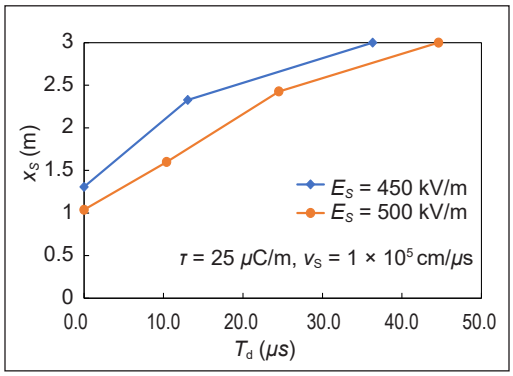

Figure 17. The effect of the voltage gradient of the streamer on discharge duration under the assumption that τ=25 μC/m, v_S=1×10^5 m/s

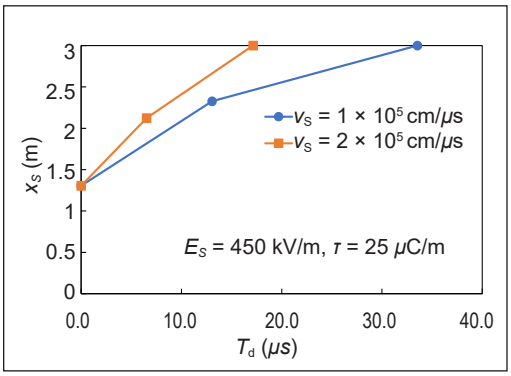

Figure 18. The effect of streamer velocity on discharge duration under the assumption that E_S=450 kV/m, τ=25 μC/m

Table 6
Simulation results of streamer-leader propagation system under the assumption that E_S=450 kV/m, τ=25 μC/m

Step	V_{app} (kV)	K_Q (μC/kV·m)	l_S (m)	Q (μC)	t (μs)	l_L (m)	v_L (×10^4 m/s)	l_R (m)	Final jump
v_S=1×10^5 m/s									
1	-1036	0.055	1.31	6.96	68.7	0.00	0.00	3.00	N
2	-1136	0.08	2.33	15.90	81.8	0.28	2.13	2.72	N
3	-1268	0.10	2.72	56.70	105.0	0.91	2.73	2.09	Y
4	-1369					3.00	7.68		Breakdown
v_S=1.5×10^5 m/s									
1	-1036	0.055	1.31	6.96	68.7	0.00	0.00	3.00	N
2	-1105	0.08	2.20	14.59	77.4	0.28	1.90	2.72	N
3	-1201	0.10	2.72	55.32	92.1	0.86	3.22	2.14	Y
4	-1291					3.00	12.35	0.00	Breakdown

Table 7
The comparison between the simulation results and the experimental results under the assumption that E_S=450 kV/m, τ=25 μC/m

Parameters	Simulation results	Experimental results (He et al., 2012)	Unit	Error (%)
		v_S=1×10^5 m/s		
V_{ini}	-1036	-1052.00	kV	-1.5
l_{SM}	2.72	2.30	m	18.3
l_F	2.09	2.30	m	-9.1
v_L	2.43	2.20	×10^4 m/s	10.5
T_d	36.3	29.7	μs	22.2
$V_{50\%}$	-1369	-1365.00	kV	0.3
		v_S=1.5×10^5 m/s		
V_{ini}	-1036	-1052.00	kV	-1.5
l_{SM}	2.72	2.30	m	18.3
l_F	2.14	2.30	m	-7.0
v_L	2.56	2.20	×10^4 m/s	16.4
T_d	23.4	29.7	μs	21.2
$V_{50\%}$	-1291	-1365.00	kV	-5.4

DISCUSSION

The leader discharge develops in a stepwise fashion. The electric field after the streamer discharge is a quasi-static electric field at each stage. Therefore, FEM is a suitable and effective method to investigate the electric field distribution in the air gap at each stage of the leader development. The electric field in the streamer zone is constant so that the discharge parameters for each stage of leader propagation can be easily calculated using FEM-VDM. The above simulation process shows that FEM-VDM can simulate the dynamic process of positive leader discharge without complex physical calculations. However, the validity of the simulation model depends on a reasonable assumption of initial parameters, such as charge density τ of the leader channel, streamer voltage gradient E_S, and streamer velocity v_S. This model successfully predicted the leader onset and breakdown voltage with small errors (Table 6). The leader velocity, the largest streamer length, and the discharge duration are close to the experiment results. It shows that the value of 450 kV/m for the voltage gradient of the streamer is suitable, which is consistent with the recent studies by Tao et al. (2022), Zixin et al. (2020), and Ping et al. (2022).

However, it should be pointed out that this model cannot accurately predict the macro parameters of leader discharge under any gap length or any electrode structure, such as breakdown voltage, leader velocity, and leader length, because the development speed of the streamer and the charge density of the leader channel are not the same for different electrode structures and different gaps (Gu et al., 2010, 2012; He et al., 2012). Different initial parameters should be matched according to different model structures when doing

simulation research. It is also a research direction in the leader discharge simulation research. The main contribution of this study is that it demonstrated that FEM-VDM could simulate the dynamic process of the leader discharge, which provides a new method for research in this field. Compared with the traditional CSM model, such as those proposed by Bondiou & Gallimberti (1994), Goelian et al. (1997), and Becerra and Cooray (2006a), FEM does not require the configuration of complex charge simulation systems and the writing of complex computer programs, thereby making the calculation process simple and efficient.

CONCLUSION

A simplified self-consistent numerical model used to simulate the dynamic process of positive leader discharge in an inverted rod-plane gap was modeled based on FEM and VDM. The voltage distortion coefficient K_Q used to calculate the streamer length and space charge was analyzed. The physical dynamic process of the positive leader discharge was simulated with the help of COMSOL Multiphysics and MATLAB co-simulation technology. The simulation results are in good agreement with the experimental results. This model is based on FEM, which can deal with arbitrary electrode configurations and complex boundary conditions. In addition, the calculation process of the model is simple without complex multiphysics computing. The above advantages make the model capable of conducting leader discharge simulation under any complex electrode configuration and arbitrary boundary conditions without simplifying the model structure, which makes the model more flexible in engineering applications than traditional CSM models, such as those proposed by Bondiou and Gallimberti (1994), Goelian et al. (1997) and Becerra and Cooray (2006a).

ACKNOWLEDGMENT

The authors thank Universiti Putra Malaysia, Malaysia, for the research funding provided for this study under the GP-IPB scheme (GP-IPB/2022/9717001) for the financial support of this research.

REFERENCES

Arevalo, L., Cooray, V., Wu, D., & Jacobson, B. (2012). A new static calculation of the streamer region for long spark gaps. *Journal of Electrostatics*, *70*(1), 15-19. https://doi.org/10.1016/j.elstat.2011.07.013

Becerra, M. (2013). Glow corona generation and streamer inception at the tip of grounded objects during thunderstorms: Revisited. *Journal of Physics D: Applied Physics*, *46*(13), Article 135205. https://doi.org/10.1088/0022-3727/46/13/135205

Becerra, M., & Cooray, V. (2006a). A simplified physical model to determine the lightning upward connecting leader inception. *IEEE Transactions on Power Delivery*, *21*(2), 897-908. https://doi.org/10.1109/TPWRD.2005.859290

Becerra, M., & Cooray, V. (2006b). A self-consistent upward leader propagation model. *Journal of Physics D: Applied Physics*, *39*(16), 3708-3715. https://doi.org/10.1088/0022-3727/39/16/028

Bondiou, A., & Gallimberti, I. (1994). Theoretical modelling of the development of the positive spark in long gaps. *Journal of Physics D: Applied Physics*, *27*(6), 1252-1266. https://doi.org/10.1088/0022-3727/27/6/024

Brezmes, A. O., & Breitkopf, C. (2014). Simulation of inductively coupled plasma with applied bias voltage using COMSOL. *Vacuum*, *109*, 52-60. https://doi.org/10.1016/j.vacuum.2014.06.012

Chen, S., He, H., Zou, Y., He, J., & Chen, W. (2016, September 19-22). *Simulation of corona space charge generated from the ±800kV UHVDC overhead transmission line in a thunderstorm*. [Paper presentation]. 2016 IEEE International Conference on High Voltage Engineering and Application (ICHVE), Chengdu, China. https://doi.org/10.1109/ICHVE.2016.7800706

Cigre, W. G. (2021). *Procedures for Estimating the Lightning Performance of Transmission Lines – New Aspects*. CIGRE.

Cooray, V. (2014). *The Lightning Flash* (2nd ed.). Institution of Engineering and Technology.

Diaz, O., Cooray, V., & Arevalo, L. (2018). Numerical modeling of electrical discharges in long air gaps tested with positive switching impulses. *IEEE Transactions on Plasma Science*, *46*(3), 611-621. https://doi.org/10.1109/TPS.2018.2802039

Ding, Y., Lv, F., Zhang, Z., Liu, C., Geng, J., & Xie, Q. (2016). Discharge Simulation of typical air gap considering dynamic boundary and charge accumulation. *IEEE Transactions on Plasma Science*, *44*(11), 2615-2621. https://doi.org/10.1109/TPS.2016.2600179

El-Zein, A., Talaat, M., & Samir, A. (2018). Positive streamer in gases: Physical approach from low to high energies. *Vacuum*, *156*, 469-474. https://doi.org/10.1016/j.vacuum.2018.07.051

Gallimberti, I., Bacchiega, G., Bondiou-Clergerie, A., & Lalande, P. (2002). Fundamental processes in long air gap discharges. *Comptes Rendus Physique*, *3*(10), 1335-1359. https://doi.org/10.1016/S1631-0705(02)01414-7

Gao, J., Wang, L., Li, G., Fang, Y., Song, B., Xiao, B., & Liu, K. (2020). Discharge of air gaps during ground potential live-line work on transmission lines. *Electric Power Systems Research*, *187*, Article 106519. https://doi.org/10.1016/j.epsr.2020.106519

Goelian, N., Lalande, P., Bondiou-Clergerie, A., Bacchiega, G. L., Gazzani, A., & Gallimberti, I. (1997). A simplified model for the simulation of positive-spark development in long air gaps. *Journal of Physics D: Applied Physics*, *30*(17), 2441-2452. https://doi.org/10.1088/0022-3727/30/17/010

Gu, J., He, K., Yu, H., Chen, W., Bian, K., & Shi, W. (2020, September 6-10). *Effect of space charge on lightning shielding performance of UHVDC transmission line under lightning downward leader.* [Paper presentation]. 2020 IEEE International Conference on High Voltage Engineering and Application (ICHVE), Beijing, China. https://doi.org/10.1109/ICHVE49031.2020.9279506

Gu, S., Chen, W., Chen, J., He, H., & Qian, G. (2010). Observation of the streamer–leader propagation processes of long air-gap positive discharges. *IEEE Transactions on Plasma Science*, *38*(2), 214-217. https://doi.org/10.1109/TPS.2009.2037004

Gu, S., Xiang, N., Chen, J., He, H., Xie, S., & Chen, W. (2012, September 2-7). *Observation of 3m rod-rod discharges under switching impulse voltage*. [Paper presentation]. 2012 International Conference on Lightning Protection (ICLP), Vienna, Australia. https://doi.org/ 0.1109/ICLP.2012.6344360

He, H., He, J., Chen, W., Xie, S., Xiang, N., Chen, J., & Gu, S. (2012). Comparison of positive leader propagation in rod–plane and inverted rod-plane gaps. *IEEE Transactions on Plasma Science*, *40*(1), 22-28. https://doi.org/ 10.1109/TPS.2011.2172002

Hnatiuc, B., Sabau, A., & Astanei, D. (2019). Classic spark simulation using COMSOL software. *IOP Conference Series: Materials Science and Engineering*, *591*, Article 012050. https://doi.org/10.1088/1757-899X/591/1/012050

Lalande, P., Bondiou-Clergerie, A., Bacchiega, G., & Gallimberti, I. (2002). Observations and modeling of lightning leaders. *Comptes Rendus Physique*, *3*(10), 1375-1392. https://doi.org/10.1016/S1631-0705(02)01413-5

Les Renardières Group. (1973). *Research on Long Air Gap Discharges at Les Renardières*. https://e-cigre.org/publication/ELT_023_3-research-on-long-air-gap-discharges-at-les-renardieres

Les Renardières Group. (1974). *Research on Long Air Gap Discharges at Les Renardières:1973 Results*. https://e-cigre.org/publication/ELT_023_3-research-on-long-air-gap-discharges-at-les-renardieres

Li, Z., Zeng, R., Yu, Z., Chen, S., Liao, Y., & Li, R. (2013). Research on the upward leader emerging from transmission line by laboratory experiments. *Electric Power Systems Research*, *94*, 64-70. https://doi.org/10.1016/j.epsr.2012.05.016

Mohammadi, R., Vahidi, B., & Rahiminejad, A. (2019). Estimation of HVDC transmission lines shielding failure using LPM method and an adapted SLIM model. *IET Science, Measurement & Technology*, *13*(9), 1345-1351. https://doi.org/10.1049/iet-smt.2018.5180

Naidu, M. S., & Kamaraju, V. (2013). *High voltage engineering*. McGraw-Hill Education (India) Pte Ltd.

Nijdam, S., Teunissen, J., & Ebert, U. (2020). The physics of streamer discharge phenomena. *Plasma Sources Science and Technology*, *29*(10), Article 103001. https://doi.org/10.1088/1361-6595/abaa05

Petrov, N. I., & Waters, R. T. (2021). Lightning to earthed structures: Striking distance variation with stroke polarity, structure geometry and altitude based on a theoretical approach. *Journal of Electrostatics*, *112*, Article 103599. https://doi.org/10.1016/j.elstat.2021.103599

Ping, W., Yaxi, C., Xiuyuan, Y., Yujian, D., Jianghai, G., Fangcheng, L., Ling, J., & Weidong, S. (2022). Transformation characteristics of large-size ball-plate gap discharge under positive polarity operating impact at an altitude of 2200m. *Chinese Journal of Electrical Engineering,* 1-11. Advance online publication. https://kns.cnki.net/kcms/detail/11.2107.TM.20220708.1730.031.html

Rizk, F. A. M. (1989). A model for switching impulse leader inception and breakdown of long air-gaps. *IEEE Transactions on Power Delivery*, *4*(1), 596-606. https://doi.org/10.1109/61.19251

Rizk, F. A. M. (2009). Modeling of proximity effect on positive leader inception and breakdown of long air gaps. *IEEE Transactions on Power Delivery*, *24*(4), 2311-2318. https://doi.org/10.1109/TPWRD.2009.2027494

Rizk, F. A. M. (2020). New approach for assessment of positive streamer penetration of long air gaps under impulse voltages. *IEEE Transactions on Dielectrics and Electrical Insulation*, *27*(3), 791-798. https://doi.org/10.1109/TDEI.2020.008588

Rodrigues, E., Pontes, R., Bandeira, J., & Aguiar, V. (2019). Analysis of the incidence of direct lightning over a HVDC transmission line through EFD model. *Energies*, *12*(3), Article 555. https://doi.org/10.3390/en12030555

Talaat, M., El-Zein, A., & Samir, A. (2019). Numerical and simulation model of the streamer inception at atmospheric pressure under the effect of a non-uniform electric field. *Vacuum*, *160*, 197-204. https://doi.org/10.1016/j.vacuum.2018.11.037

Tao, Y., Xiaotian, W., Wenxia, S., & Ming, Y. (2022). Space charge criterion of the initial streamer for the stable inception of positive upleader under lightning strikes. *Chinese Journal of Electrical Engineering*, 1-13. Advance online publication. https://kns.cnki.net/kcms/detail/11.2107.tm.20220419.1016.004.html

Wang, X., He, J., Yu, Z., Zeng, R., & Rachidi, F. (2016). Influence of ground wire on the initiation of upward leader from 110 to 1000 kV AC phase line. *Electric Power Systems Research*, *130*, 103-112. https://doi.org/10.1016/j.epsr.2015.08.022

Xu, Y., & Chen, M. (2013). A 3-D self-organized leader propagation model and its engineering approximation for lightning protection analysis. *IEEE Transactions on Power Delivery*, *28*(4), 2342-2355. https://doi.org/10.1109/TPWRD.2013.2263846

Yang, N., Zhang, Q., Hou, W., & Wen, Y. (2017). Analysis of the lightning-attractive radius for wind turbines considering the developing process of positive attachment leader: Attractive radius for wind turbines. *Journal of Geophysical Research: Atmospheres*, *122*(6), 3481-3491. https://doi.org/10.1002/2016JD026073

Zeng, R., Li, Z., Yu, Z., Zhuang, C., & He, J. (2013). Study on the influence of the dc voltage on the upward leader emerging from a transmission line. *IEEE Transactions on Power Delivery*, *28*(3), 1674-1681. https://doi.org/10.1109/TPWRD.2013.2252371

Zhou, Q., Liu, C., Bian, X., Lo, K. L., & Li, D. (2018). Numerical analysis of lightning attachment to wind turbine blade. *Renewable Energy*, *116*, 584-593. https://doi.org/10.1016/j.renene.2017.09.086

Zixin, G., Qingmin, L., Wanshui, Y., Hongbo, L., Li, Z., & Wah Hoon, S. (2020). The dynamic critical length criterion of initial streamer for the stable upward leader inception under negative lightning strikes. *Proceedings of the CSEE*, *40*(5), 1713-1721. https://doi.org/10.13334/j.0258-8013.pcsee.190881